A novel method to accurately estimate pathway activity in single cells for clustering and differential analysis

Daniel Davis, Avishai Wizel, Yotam Drier

The Lautenberg Center for Immunology and Cancer Research, IMRIC, Faculty of Medicine, Hebrew University of Jerusalem, Israel.

Abstract

Inferring which and how biological pathways and gene sets are changing is a key question in many studies that utilize single-cell RNA sequencing. Typically, these questions are addressed by quantifying the enrichment of known gene sets in lists of genes derived from global analysis. Here we offer a new method to first infer pathway activity in each cell. This allows more sensitive differential analysis and utilizing pathway scores to cluster cells and compute UMAP or other similar projections. We apply our method on datasets of COVID-19 and glioblastoma, and demonstrate its utility. SiPSiC analysis is consistent with findings reported by previous analyses in many cases, but also reveals the differential expression of novel pathways, enabling us to suggest new mechanisms underlying the pathophysiology of these diseases and demonstrating SiPSiC's high accuracy and sensitivity in detecting biological function and traits. In addition, we demonstrate how it can be used to better classify cells based on activity of biological pathways instead of single genes and its ability to overcome patient specific artifacts.

Introduction

Single-cell RNA sequencing (scRNA-seq) has been in widespread use for several years, enabling us to deepen our understanding of tissue characteristics and heterogeneity in health and disease (Chi & Deng, 2020). Pathway analysis has proven to be a useful tool to interpret gene expression data in general and scRNA-seq in particular. This is typically accomplished by identifying a set of interesting genes (such as differentially expressed genes) and then determining which pathways these genes are over-represented in. While such approaches are very useful, there are many potential benefits to estimate pathway activity in each cell first and then utilize this information for downstream analysis. Such an approach allows for both overcoming limitations of single-cell data, such as inaccurate estimation of the expression of a single gene in a single cell, and utilizing pathway activity for unsupervised analysis such as clustering. We and others have developed approaches for pathway analysis in single sample for bulk RNA-seq (Drier et al., 2013; Hänzelmann et al., 2013; H. Wang et al., 2016), however methods developed for bulk RNA-seq often do not work well for scRNA-seq data, due to its special characteristics (Noureen et al., 2022).

The most prominent method that can be utilized to estimate pathway activity in single cells is AUCell (Aibar et al., 2017). AUCell was originally developed as part of an effort to reconstruct gene regulatory networks, but it allows to score gene sets in the process. To do so, it ranks all the genes expressed by a cell based on their expression level and uses the area under the curve (AUC) measure to represent the fraction of the top 5% genes which belongs to the relevant gene set. While AUCell helped in the analysis of several scRNA-seq studies, it suffers from several limitations, including inability to calculate meaningful score if most genes in the gene set are not highly expressed, inaccuracy in scoring small gene sets, and lower sensitivity in picking up subtle changes.

Here we present Single Pathway analysis in Single Cells (SiPSiC), a novel method for analyzing the activity of a gene set, or biological pathway, in single cells. SiPSiC reaches high sensitivity by relying on the normalized expression of all genes, and not just the ranking of the most highly expressed ones. Using SiPSiC, we reanalyze scRNA-seq data of COVID-19 and glioblastoma, identify known and new

cellular pathways involved in these diseases, and demonstrate SiPSiC's high accuracy and superior ability to identify changes in pathway activity missed by the original analyses. Moreover, we suggest new ways to cluster and visualize the data based on SiPSiC scores, which reduces typical biases of single gene analysis and emphasizes similarity based on shared biological processes.

Results

A new tool to infer pathway activity in single cells

As scRNA-seq data is typically sparse due to a high drop-out rate, elaborate pathway analysis developed for bulk gene expression assays suffers from low accuracy. We therefore developed SiPSiC, a new tool to calculate pathway scores for each cell and each gene set by using gene expression values normalized both by the expression levels in other cells and by the rank of the average gene expression across all genes (see Methods). These two normalizations are the major factors allowing us to robustly estimate pathway activity, even in small datasets where few cells exist or many of the pathway genes are lacking.

Available on both GitHub and Bioconductor, SiPSiC is an easily installed and well documented tool to dissect single cell level differences with unprecedented accuracy, allowing its users to interrogate tissue physiology and heterogeneity with high sensitivity and accuracy.

SiPSiC reveals differential activity of hallmark pathways with potential therapeutic implications in rare or small populations of COVID-19 infected cells

We used SiPSiC to study changes in activity of biological pathways after SARS-CoV-2 infection in two distinct datasets: single nuclei RNA-seq of recently deceased COVID-19 patients or control lung tissues sampled before the outbreak of COVID-19 (Melms et al., 2021) and scRNA-seq of African green monkeys shortly after infection with SARS-CoV-2 or inactivated virus (Speranza et al., 2021). The original analysis of the human data included gene-based clustering from which cluster markers were inferred to elucidate cellular response to SARS-CoV-2 infection. The monkey data was originally analyzed by principal component analysis (PCA), clustering and Fast Gene Set Enrichment Analysis (Korotkevich et al., 2021). We calculated pathway scores per cell for each of the 50 MSigDB hallmark gene sets (Liberzon et al., 2015). We then compared pathway scores between SARS-CoV-2 positive and negative controls and calculated the difference between the groups' median scores, for each pathway. A pathway was considered up- or down-regulated in one group compared to another if in their comparison we got a false discovery rate (FDR) < 0.01 and a positive or negative median difference, respectively. Our findings can be largely divided into three categories: 1) Innate immune response of pneumocytes; 2) Pathways modulated by the virus to support its life cycle; and 3) Adaptive immune response in B and CD8+ T cells.

First, we applied SiPSiC to human alveolar cells (of both type 1 and 2; 4575 cells from COVID-19 patients vs 4303 control cells). 12 out of 50 pathways were downregulated in COVID-19 patients, and 31 upregulated (t-test, FDR < 0.01, Figure 1A; see Supplementary Table S1). In addition to interferon response which was also reported as upregulated in alveolar type 2 (AT2) cells by Melms et al., we identified many more upregulated pathways involved in innate immune response and its implications, among them are genes involved in the complement pathway, DNA repair and WNT/β catenin signaling. Indeed, the complement system was shown to be hyperactivated in severe SARS-CoV-2 infections (Afzali et al., 2021), SARS-CoV-2 induces DNA damage (Gioia et al., 2023), and wnt5a is upregulated in severe cases of COVID-19 (Choi et al., 2020). We also found upregulation of the mitotic spindle (FDR < $1.1*10^{-4}$) and E2F targets (FDR < $2.3*10^{-15}$), which is consistent with demonstrated hyperplasia of pneumocytes in humans and monkeys post SARS-CoV-2 infection (Ackermann et al., 2020; Speranza et al., 2021). In addition, Melms et al. found that the alveolar cells of the COVID-19

group showed lower expression of the ETV5 transcription factor required for maintaining AT2 cell identity compared to alveolar cells of the control lungs. Combined, these findings suggest that infected pneumocytes try to compensate for the damaged tissue by advancing the cell cycle and differentiating towards AT1 cells. Furthermore, SiPSiC detected upregulation of the hallmark apoptosis pathway (FDR < 10^{-30}), consistent with detection of many apoptotic cells in human airway epithelium cultures infected with SARS-CoV-2 (Zhu et al., 2020). This may relate to apoptosis induction by the viral ORF3a protein (Ren et al., 2020). Additionally, it may relate to apoptosis induction by p53, and indeed SiPSiC also detected upregulation of the p53 pathway (FDR < $8.1 * 10^{-133}$). Prior research showed that viral infection upregulates p53 by type 1 interferon signaling (Takaoka et al., 2003) and, on the other hand, that p53 both activates the interferon pathway and promotes type 1 interferon release from cells undergoing viral infection (Muñoz-Fontela et al., 2008). These findings together suggest this positive feedback loop of interferon and p53 may also play a role in SARS-CoV-2 infection.

In the category of pathways modulated by the virus to support its life cycle, SiPSiC found upregulation of the PI3K/AKT/mTOR and mTORC1 pathways, consistent with evidence that these pathways are activated after SARS-CoV-2 infection (Appelberg et al., 2020). Moreover, mTORC1 activation is known to induce expression of key enzymes involved in several metabolic pathways, among them are glycolysis and biosynthesis of fatty acids and cholesterol (Düvel et al., 2010), supporting SiPSiC's findings that the glycolysis, fatty acid metabolism and cholesterol homeostasis were all upregulated in the alveolar cells of COVID-19 patients. Further support for the upregulation of glycolysis is provided by previous works showing that SARS-CoV-2 infection indeed increases glycolysis, both in colon carcinoma cells and in monocytes (Bojkova et al., 2020; Codo et al., 2020). Importantly, mTORC1 was also shown before to activate the IRE1-JNK signaling pathway of the unfolded protein response (UPR), thereby triggering apoptosis (Kato et al., 2012). SiPSiC found that the UPR pathway was upregulated too (FDR < $1.18 * 10^{-68}$), consistent with the activation of mTORC1 and previous research suggesting that SARS-CoV-2 induces the unfolded protein response (Echavarría-Consuegra et al., 2021). Interestingly, a previous review stated that UPR activation can increase type 1 interferon production (Sprooten & Garg, 2020). Combined, all these findings suggest that SARS-CoV-2 infection increases endoplasmic reticulum (ER) stress and UPR activation which are also enhanced by the viral-induced upregulation of mTORC1, thereby promoting apoptotic cell death and possibly also the positive feedback loop involving P53 and type 1 interferons, which further encourages apoptosis. Another pathway in this category which was found upregulated consists of genes upregulated by reactive oxygen

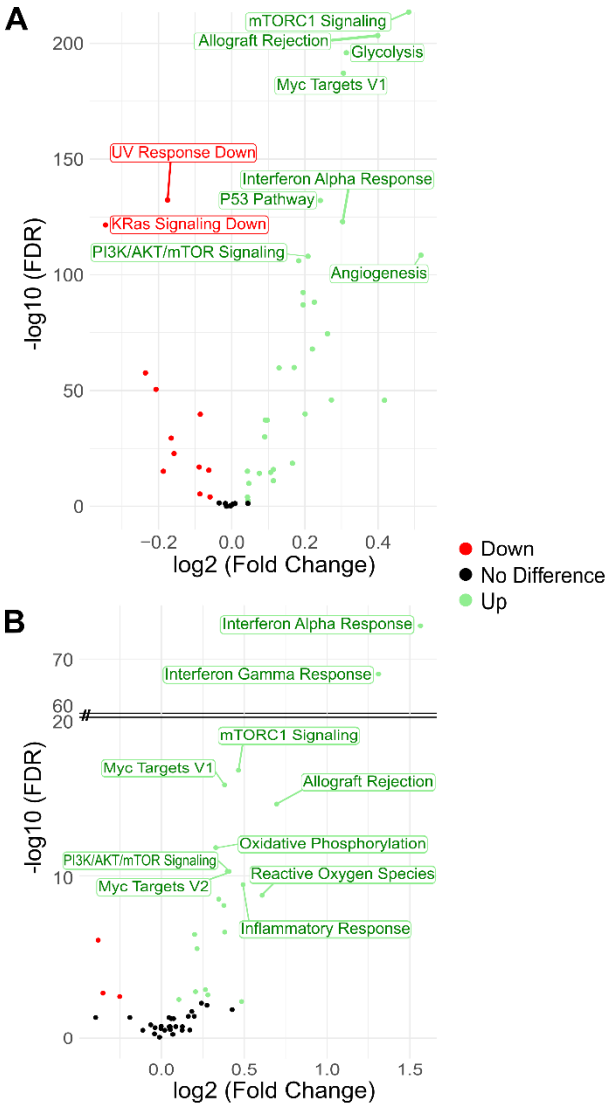

Figure 1. Volcano plots showing differentially expressed Hallmark pathways in COVID-19 infected alveolar cells according to SiPSiC analysis. Top significant pathways are labeled. (**A**) The human dataset. (**B**) The African green monkey dataset (The active infection group compared to control).

species (ROS). Oxidative stress is known to be induced by several viruses (Lee, 2018), and monocytes infected with SARS-CoV-2 showed higher production of mitochondrial ROS (Codo et al., 2020), suggesting that SARS-CoV-2 also induces oxidative stress in the infected cells. Together, these results suggest that SARS-CoV-2 activates mTOR and induces glycolysis and oxidative stress.We applied SiPSiC on human activated B cells (55 cells of COVID-19 patients, 48 control cells) and CD8+ T cells (103 COVID-19 cells, 6 control) to better characterize the adaptive immune response. Despite the relatively small cell populations, TGF Beta signaling was found upregulated in activated B cells of COVID-19 patients (FDR < 0.006), consistent with previous reports (Ferreira-Gomes et al., 2021; Melms et al., 2021). The G2M checkpoint pathway was upregulated in the CD8+ T cell group of COVID-19 patients (FDR < 0.003), a finding missed by the conventional analysis in Melms et al., but consistent with the expected increase in T cell proliferation in the lungs (Liao et al., 2020). The interferon gamma response pathway was found upregulated in the SARS-CoV-2 infected CD8+ T cells as well, albeit with borderline statistical significance (FDR < 0.032). This finding is well correlated with prior evidence of elevated interferon levels in the plasma of COVID-19 patients and the resulting effect on immune cells, and with previous evidence showing upregulation of interferon-related genes across different types of immune cells collected from the mediastinal lymph nodes of SARS-CoV-2 infected monkeys (Schultheiß et al., 2020; Speranza et al., 2021).

Importantly, many of the pathways that SiPSiC found as upregulated in the alveolar cells of the COVID-19 group demonstrated therapeutic potential, including DNA repair, UPR, PI3K/AKT/mTOR, ROS and metabolic pathways. Drugs targeting DNA damage response can block SARS-CoV-2 replication (Garcia et al., 2021), suggesting that SARS-CoV-2 not only increases DNA damage in the infected cells, but also relies on the cells' reaction to it. SARS-CoV-2 replication can be blocked by UPR inhibitors (Echavarría-Consuegra et al., 2021), PI3K/AKT/mTOR inhibitors (Appelberg et al., 2020; Klann et al., 2020; Stukalov et al., 2021; Yuen et al., 2021), and drugs targeting lipid metabolism (Abu-Farha et al., 2020; Williams et al., 2021). Treatment of COVID-19 patients with N-Acetylcysteine (NAC), a precursor of the antioxidant agent glutathione, was found correlated with lower mortality in a retrospective study (Izquierdo et al., 2022), and SARS-CoV-2 infected monocytes treated with antioxidant agents such as NAC showed reduction in both viral replication and production of several cytokines, in particular interferons of types 1 and 2 (Codo et al., 2020). Codo et al. further showed that the increased production of ROS in infected monocytes promotes glycolysis, and that inhibitors of glycolysis also reduced SARS-CoV-2 replication and could reduce the production of type 1 and 2 interferons. Notably, glycolysis inhibitors also reduced SARS-CoV-2 replication in colon carcinoma cells (Bojkova et al., 2020).

Together this suggests that mTOR signaling and impact on ROS and metabolism play an important role in the pathophysiology of COVID-19, and drugs targeting several of these pathways could have synergistic effects with consequences on disease progression and severity.

In the African green monkey experiment, two monkeys were inoculated with inactivated SARS-CoV-2 (henceforth referred to as control) and eight with the active virus (Speranza et al., 2021). To better study the dynamics of viral infection, these eight monkeys were then split into two groups of four monkeys each and euthanized three (first group) or ten (second) days post inoculation, where the monkeys in the 10 days group had already recovered by the 10th day. Hence, we focused on comparing the active infection (3-days) to the control after calculating the pathway scores per cell type (Methods). Complete results of all three groups can be found in Supplementary Table S2.

Analysis of this dataset provided support for pathways that were found upregulated from all three categories. We found 20 upregulated and 3 downregulated pathways in alveolar cells (Figure 1B). Here too the cells in the active infection group were enriched in the interferon alpha and gamma response, complement, E2F targets and apoptosis pathways relative to both other groups (Supplementary Table S2), supporting our findings from the analysis of human alveolar cells. Importantly, most of the pathways showing therapeutic potential that were found upregulated in the COVID-19 group of alveolar cells in the human dataset were also upregulated in the alveolar cells of the active infection

group in the monkey dataset, compared to control. These are the DNA repair, mTORC1 and PI3K/AKT/mTOR signaling, glycolysis, reactive oxygen species and unfolded protein response pathways. Out of all these pathways, only interferon signaling was identified by Speranza et al., further highlighting SiPSiC's high sensitivity.

Analysis of the immune cells that were found in the monkeys' lungs revealed that in both the B and CD8+ T cells, the interferon alpha and gamma response pathways were enriched in the 3-days group, in concordance with our finding of interferon gamma upregulation in CD8+ T cells from the human dataset and the evidence showing elevated interferon levels in the plasma of COVID-19 patients and its consequences on immune cells (Schultheiß et al., 2020; Speranza et al., 2021). In addition, both MYC target pathways (V1 and V2) were found upregulated in the active infection (3-days) group of the CD8+ T cells compared to control. We indeed expect to see upregulation of MYC targets in T cells, since MYC is known to be involved in T cell proliferation (Gnanaprakasam & Wang, 2017), and increased T cell proliferation occurs in COVID-19 patients' lungs (Liao et al., 2020). To ascertain this finding, we compared MYC expression in the control and active infection groups. Indeed, average MYC expression 3 days after infection was 89% higher than control ($p < 0.0032$, unpaired Wilcoxon test), strongly supporting SiPSiC's finding. Furthermore, the inflammatory response pathway was also enriched in the 3-days group of CD8+ T cells, reflecting the anti-viral activity.

Remarkably, SiPSiC also found the upregulation of the IL6/JAK/STAT3 signaling pathway in the active infection group of CD8+ T cells compared to control (FDR < $5.72 * 10^{-9}$), a finding supported by evidence for high levels of IL-6 in the serum of COVID-19 patients even in relatively mild cases and increased IL-6 secretion from epithelial cells infected with SARS-CoV-2 (Han et al., 2020; Patra et al., 2020; Sanli et al., 2021). This is another example for SiPSiC's potential to highlight therapeutically relevant pathways, as the IL-6/JAK/STAT3 signaling pathway has been suggested as a therapeutic target for COVID-19 (Jafarzadeh et al., 2021). Similarly, the notch signaling pathway was found upregulated in this group, although with borderline statistical significance (FDR < 0.034). Notch too was suggested as a therapeutic target in COVID-19 before, as it is known to modulate the immune response and is involved in a positive feedback loop with IL-6 expression in macrophages (Rizzo et al., 2020). This suggests that CD8+ T cells may exhibit the same feedback loop upon SARS-CoV-2 infection, and that IL-6 signaling could be moderated in these cells by inhibiting notch signaling.

<u>SiPSiC analysis of glioblastoma cell subpopulations reveals novel differentially expressed pathways showing further potential therapeutic implications</u>

To validate the applicability of SiPSiC to different data types, we analyzed scRNA-seq data of glioblastoma tumors (Neftel et al., 2019). In their work Neftel et al. identified four malignant meta-modules (cellular states): Oligodendrocyte-progenitor-like (OPC-like), neural-progenitor-like (NPC-like), astrocyte-like (AC-like) and mesenchymal-like (MES-like). We calculated pathway scores per cell (n = 6,576) for each of the same 50 hallmark pathways (Supplementary Table S3). The cells were then split into four groups based on their cell state assignments (1,986 NPC-, 1,047 OPC-, 1,929 AC- and 1,614 MES-like cells), and comparisons were made between each pair of groups. We found that the G2M checkpoint pathway was upregulated in the OPC- and NPC-like groups compared to the AC- and MES-like groups, indicative of a higher proportion of proliferating cells in these cell states. In addition, the hypoxia response pathway was enriched in the MES-like group compared to all other three groups. These findings are consistent with the findings reported in Neftel et al. Furthermore, SiPSiC analysis suggests that the MES-like group was enriched in the inflammatory response pathway, in concordance with prior evidence that the mesenchymal subtype of GBM tumors is enriched in inflammatory response associated genes (Engler et al., 2012).

Importantly, SiPSiC analysis of the glioblastoma dataset also pointed out pathways with therapeutic implications. The TGFβ (FDR< $5*10^{-14}$), TNFα via NFκB (FDR< $2.9*10^{-117}$) and IL-6/JAK/STAT3 (FDR<

$9.1*10^{-36}$) signaling pathways and the epithelial to mesenchymal transition (EMT) pathway (FDR< $1.1*10^{-113}$) were all found upregulated in the MES-like group. A previous work has shown that in gliomas, regulatory T cells secrete TGFβ and thereby promote the NFκB-IL-6-STAT3 signaling axis, and that IL-6 receptor blockers have a potential therapeutic effect (Liu et al., 2021). TGFβ signaling also activates TNFα signaling via NFκB in glioblastoma, which in turn induces mesenchymal transition (Bhat et al., 2013; Yan et al., 2022). Furthermore, these works also suggest that these two pathways can be targeted to improve overall survival and specifically attenuate resistance to radiotherapy in glioblastoma patients. Of relevance, the mesenchymal subtype of glioblastoma is correlated with high levels of both immune markers and infiltration of immune cells (Verhaak et al., 2010; Q. Wang et al., 2017). Together, these findings suggest that regulatory T cells infiltrate glioblastoma tumors, promoting the TGFβ, TNFα via NFκB and IL-6/JAK/STAT3 signaling pathways and thereby increasing mesenchymal transition of tumor cells.

Furthermore, SiPSiC detected up- and downregulation of the KRas signaling up (FDR < $9.8 * 10^{-22}$) and down (FDR < $1.7 * 10^{-8}$) pathways, respectively, in the MES-Like group, indicative of KRas signaling activation in it. These findings are consistent with Ras and TGFβ cooperating to induce EMT in epithelial cells and evidence that KRas activation in glioblastoma cells induces a mesenchymal shift (Kim et al., 2014; Marques et al., 2021; Zhao et al., 2021). SiPSiC also identified upregulation of ROS in the MES-like group compared to all other groups (FDR < $1.07 * 10^{-57}$), suggesting that the promotion of TGFβ-induced EMT by Ras is mediated by enhanced production of reactive oxygen species, as was shown in mammary epithelial cells (Kim et al., 2014). Taken together, our findings suggest a synergistic effect in glioblastoma where regulatory T cells activate TGFβ signaling leading to EMT which is enhanced by Ras activation. Remarkably, Ras inhibition was shown fatal to glioblastoma cells (Blum et al., 2005). Hence, our analysis suggests that a combined therapy targeting Ras and TGFβ or their downstream targets could have a synergistic therapeutic effect for glioblastoma, again demonstrating the potential of SiPSiC analysis to accelerate the development of targeted therapy.

Garofano et al. classified the cells into four distinct cell clusters: glycolytic/plurimetabolic (GPM), mitochondrial (MTC), neural (NEU) and proliferative/progenitor (PPR) (Garofano et al., 2021). They found that the GPM and MTC clusters were enriched in cells of the MES- and AC-like cell states, respectively, while the PPR and NEU clusters were enriched in cells of both the OPC- and NPC-like states. Gene set enrichment of these clusters is reported for 40 hallmark pathways, and we compared their results to SiPSiC's. 31 out of the 40 pathways (78%) were consistent, in the sense that if a pathway was reported as upregulated in one of Garofano et al. cell clusters, SiPSiC also found it is upregulated in the same cell state this cell cluster is enriched in. For instance, Garofano et al. reported that the DNA repair pathway was upregulated in the PPR cell cluster, which is enriched in both OPC- and NPC-like cells. Indeed, SiPSiC found this pathway was upregulated in both the OPC- and NPC-like cell states. Furthermore, out of the 9 other pathways eight were found by Garofano et al. to be enriched in the MTC cluster, hence we expected them to be upregulated in the AC-like cell state in our analysis. 7 of these pathways were found to be "near-consistent" in the sense that they were significantly upregulated in the AC-like cell state compared to two of the other three cell states and insignificantly either up- (5 pathways) or down-regulated (2 pathways) in it compared to the third other cell state, making 38 of the 40 (95%) pathways reported by Garofano et al. either completely or near consistent in our SiPSiC analysis.

The two remaining pathways are the hallmark notch and mTORC1 signaling pathways. Interestingly, while Garofano et al. found that the MTC cluster was enriched in the hallmark notch signaling pathway (reported FDR < $1.23*10^{-3}$), SiPSiC analysis found that it was upregulated in the OPC-like cell state (FDR < 0.0095). Although Neftel et al. did not report upregulation of notch in any of the cell states, AUCell supported SiPSiC's result finding notch upregulation in the OPC-like cell state (Supplementary Table S3). Importantly, prior research has shown that notch signaling activation inhibits the maturation and may enhance the proliferation of oligodendrocyte progenitor cells (John et al., 2002; C. Wang et al., 2017; S. Wang et al., 1998), suggesting that notch upregulation in OPC-like glioblastoma cells may play

similar roles in the pathophysiology of the disease. Similarly, while Garofano et al. found that the mTORC1 signaling pathway was enriched in the PPR cluster (reported FDR < $1.26*10^{-3}$) and Neftel et al. did not report its upregulation in any of the cell states, SiPSiC found that it was upregulated in the MES-like cell state (FDR < $3.2*10^{-75}$), again supported by AUCell which also found the same (Supplementary Table S3). Prior research has found that in epithelial cells, TGFβ-induced EMT both promotes and requires the activation of the PI3K/AKT/mTOR pathway, and more specifically activates the mTORC1 complex (Lamouille et al., 2014). Importantly, the same has also been suggested for an EMT-like process in glioblastoma (Iser et al., 2017; Zhang et al., 2014). Intriguingly, SiPSiC found the upregulation of the PI3K/AKT/mTOR signaling pathway in the MES-like cell state, in addition to the upregulation of the TGFβ signaling and EMT which were mentioned above (with all three findings also supported by AUCell, see Supplementary Table S3). Combined, these findings may well account for upregulation of the mTORC1 signaling in this cell state, supporting our finding over what Garofano et al. reported for this pathway.

To conclude, SiPSiC differential pathway analyses of the COVID-19 and glioblastoma datasets demonstrate that SiPSiC can accurately detect key differentially expressed pathways even in sparse datasets with few cells or when many of the pathways' genes are not available in the data. This allows for comprehensive and sensitive pathway analysis in single cells, that can serve to study fundamental biology as well as generate clinically and therapeutically relevant hypotheses, that may be missed by standard analysis.

Unsupervised clustering by SiPSiC reveals benign and malignant glioblastoma clones

Unsupervised clustering of scRNA-seq datasets allows to demarcate different coexisting cell lineages and subpopulations, and has thus been extensively used to interrogate tissue heterogeneity in many contexts. To test if clustering based on SiPSiC pathway scores can improve the gold standard of clustering by gene expression, we calculated cell clusters and Uniform Manifold Approximation and Projection (UMAP) of 16201 glioblastoma cells (Neftel et al., 2019), both by gene expression and by the cells' SiPSiC scores (Methods).

Gene-based clustering produced 21 clusters. Although the dataset was sampled from 9 different patients, 4 clusters consisted only of a single patient's cells, and in 7 others 95% of the cells or more were of a single patient, reflecting the strong patient-bias of the results. In contrast, using SiPSiC's scores the same analysis produced 11 clusters, with 9 of them consisting of cells from all the patients and two much smaller clusters (274 and 77 cells out of 16,201 total) where 84% and 96% of the cells were of a single patient, respectively (Figure 2A-B). These results suggest that SiPSiC based clustering was largely based on similar biological traits of the cells rather than patient identity. To validate this, we identified differential pathways in each cluster, inferred putative lineages of the different clusters, and finally tested marker genes of each cell type across the clusters for confirmation (Methods).

Cluster 3 was enriched in five immune-related gene sets: TNFA signaling via NFKB, inflammatory response, interferon alpha response, IL-6/JAK/STAT3 signaling and interferon gamma response. As the immune cells present in the dataset were macrophages and T cells, we expected this cluster to be enriched in at least one of these cell types. Testing it for enrichment in both the macrophage and T cell markers, we found that out of 2118 cells assigned to this cluster 2024 (95%) were immune cells (1960 macrophages and 64 T cells), highlighting SiPSiC's ability to detect the major biological function of cells when applied with a broad set of pathways. Two adjacent clusters on the UMAP projection (1, 6) contain 3217 additional macrophages, forming a well isolated group of 91% of the macrophages (Figure 2C). In addition, out of 150 T cells that were found in the data, 72 were assigned to the adjacent cluster 1 and formed a clearly distinct group on the UMAP (Figure 2D).

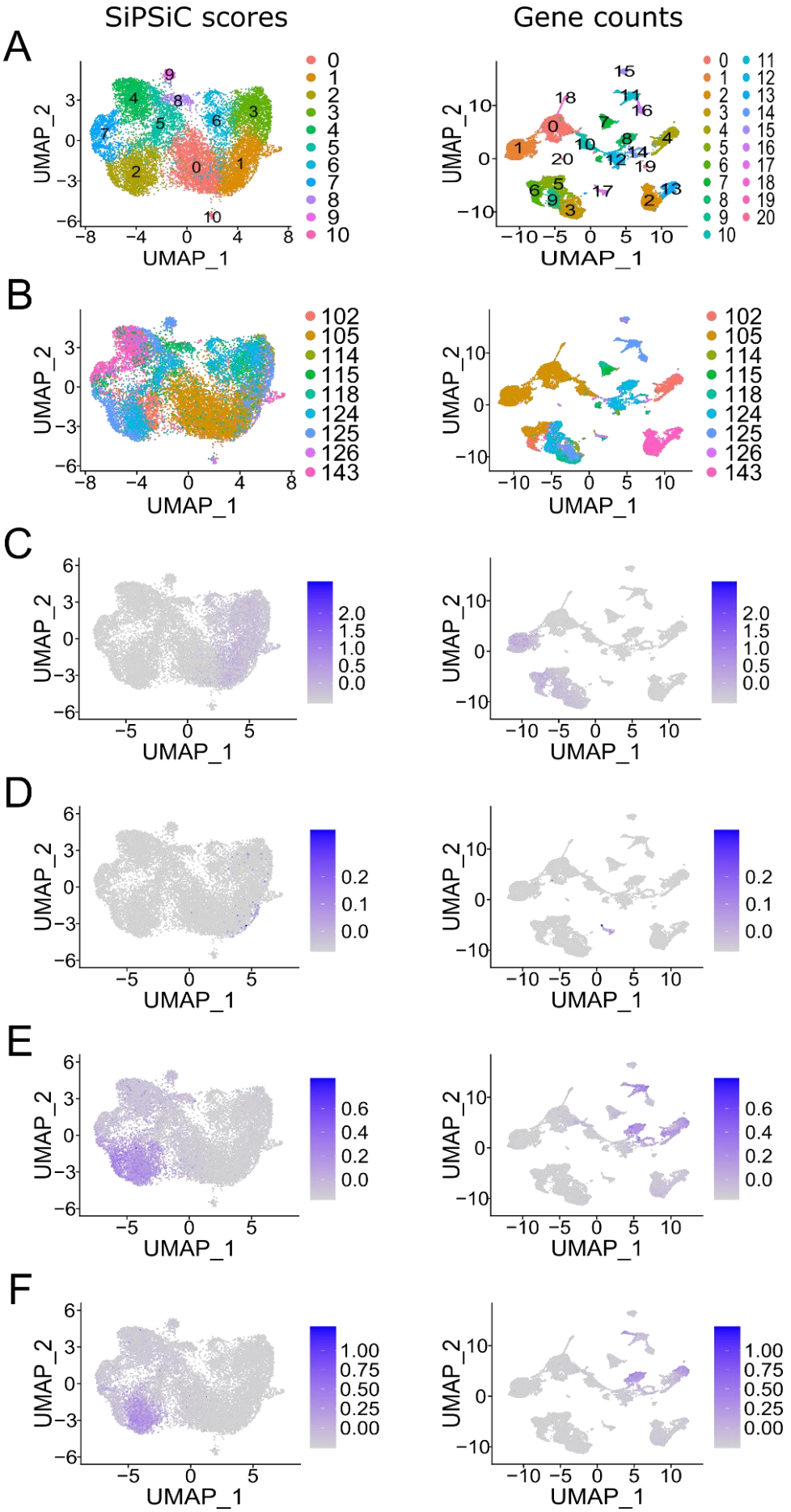

Figure 2. UMAP projections based on hallmark pathway scores by SiPSiC (left) and gene counts (right). (**A**) Cells were clustered by Louvain algorithm either according to SiPSiC scores or to gene counts. UMAPs show cells colored by cluster. (**B**) Cells colored by patient identity. (**C-F**) Marker gene set scores were calculated by SiPSiC and cells were colored according to the scores of macrophages (C), T cells (D), first (E) and second (F) NPC-like cells.

Cluster 2 demonstrated enrichment of Wnt-beta-catenin signaling and hedgehog signaling. As both pathways were found by SiPSiC to be highly enriched in the NPC-like cells in the analysis of the first glioblastoma dataset (FDR < $1.5*10^{-20}$ for the Wnt pathway and FDR < $3.5*10^{-31}$ for the hedgehog), we tested the cluster for enrichment in two different marker gene sets of this meta-module (see Methods). Out of 2380 cells assigned to this cluster 2093 (88%) and 1533 (64%) were NPC-Like cells, and these are 80% and 84% of all the NPC-Like cells in the data, according to the first and second NPC-Like markers, respectively (Figure 2E-F). These results again demonstrate SiPSiC's high accuracy.

Testing the gene-based clusters for enrichment in the same marker gene sets, we found that T cells are well clustered here as well (97% of T cells were in cluster 17). However, the macrophages were split into two main groups: One group consists of clusters 3, 5, 6 and 9, containing 3978 out of a total of 5667 macrophages (70%). 88.5% - 100% of the cells in each cluster are identified as macrophages. However, cluster 1 contains 1579 additional macrophages, which are approximately 28% of all the macrophages in the data. Notably, nearly all the cells in this cluster belong to a single patient (1717 out of 1718 cells), again showing strong patient bias that hinders the ability to cluster the cells properly, even for drastic differences such as the difference between glioblastoma cells and macrophages (Figure 2C).

Moreover, NPC-like glioblastoma cells are even more scattered across different clusters. Here, no more than 41% of the NPC-like cells in the data were assigned to a single cluster (according to either of the two marker gene sets). While about 90% of NPC-like cells (2343/2605 for NPC1, 1714/1822 for NPC2) fall in four distinct clusters (0, 4, 8 and 11), the clusters are determined by patient identity - 99.8%, 97.7%, 99.6% and 100% of the cells in clusters 0, 4, 8 and 11 each belong to a single patient, respectively (Figure 2 panels B, E, F). In particular 98% of cells in cluster 0 are not NPC-like, demonstrating the strong patient bias.

Gene expression based clustering of malignant cells is known to be driven by patient of origin, as was also observed in glioblastoma (Neftel et al., 2019). This phenomenon may help differentiate malignant from normal cells, but hinders sub-clustering of malignant cells. Here we show that SiPSiC based clustering can capture shared biological processes and be less affected by patient identity, improving the ability of clustering to robustly capture various non-malignant cell types, and importantly also shared features of different malignant cells across patients.

Pathway scoring methods benchmarking reveals higher accuracy of SiPSiC for different data types

AUCell is a common, well-established method for calculating pathway scores for each cell from scRNA-seq data. To compare SiPSiC and AUCell we used AUCell to calculate scores for the hallmark gene sets using the same three datasets above. To guarantee integrity of the results, the same preprocessing steps were applied and cell assignments to the different groups were kept.

Summary of the numbers of differentially expressed pathways found in the analysis of the monkey COVID dataset both by SiPSiC and AUCell can be found in Table 1. Overall, SiPSiC and AUCell agree on many of the differential pathways, but SiPSiC recovers more upregulated pathways. For example, SiPSiC showed clear upregulation of the complement pathway in alveolar cells undergoing active SARS-CoV-2 infection (the 3-days group, FDR < $3.7*10^{-7}$ relative to control), while AUCell failed to achieve a statistically significant result for this pathway (Figure 3A). Another compelling example is the interferon pathways in B cells, where SiPSiC showed upregulation of both the interferon alpha and gamma pathways in the 3-days group compared to the two other groups (FDR < $8.3*10^{-5}$ and FDR < 0.0009 compared to control for the interferon alpha and gamma pathways, respectively), while AUCell's analyses of these pathways failed to show a significant difference between the active infection group (3-days) and the control group (Figure 3B-C). Testing for differences in the analysis of CD8+ T cells, the MYC targets pathways came up. While SiPSiC found upregulation of both the MYC targets V1 and V2 pathways in the 3-days group compared to the control group, AUCell produced a

similar result only for the MYC targets V1 pathway, whereas a median score of zero was produced for all groups in the MYC targets V2 pathway (Figure 3D). As mentioned above, CD8+ T cell proliferation can be expected in the lungs of COVID-19 patients, and a significantly higher (89%) average MYC expression was indeed found in the active infection group compared to control in this dataset ($p < 0.0032$, unpaired Wilcoxon test), supporting SiPSiC's findings over the analysis of AUCell.

Furthermore, AUCell detected 4 pathways as downregulated in the CD8+ cells, of which none were found downregulated by SiPSiC, including the UPR and P53 pathways. Upon activation, T cells show higher absolute numbers and a higher proportion of cell surface GRP78 (sGRP78) positive cells, a marker of ER stress, and severe COVID-19 patients show higher proportions of sGRP78+ T cells and higher expression of GRP78 by pneumocytes and lung resident macrophages (Angeles-Floriano et al., 2023; Puzyrenko et al., 2021), suggesting SARS-CoV-2 infection induces the unfolded protein response in several cell types and particularly circulating T cells. Of note, SiPSiC found the UPR pathway is instead upregulated in the active infection group of CD8+ T cells, although with borderline significance (FDR < 0.071). Similarly, previous research showed higher expression of P53 in peripheral blood mononuclear cells of COVID-19 patients (Bordoni et al., 2021), suggesting that in COVID-19 T lymphocytes are likely to show higher expression of P53, again contrasting AUCell's finding.

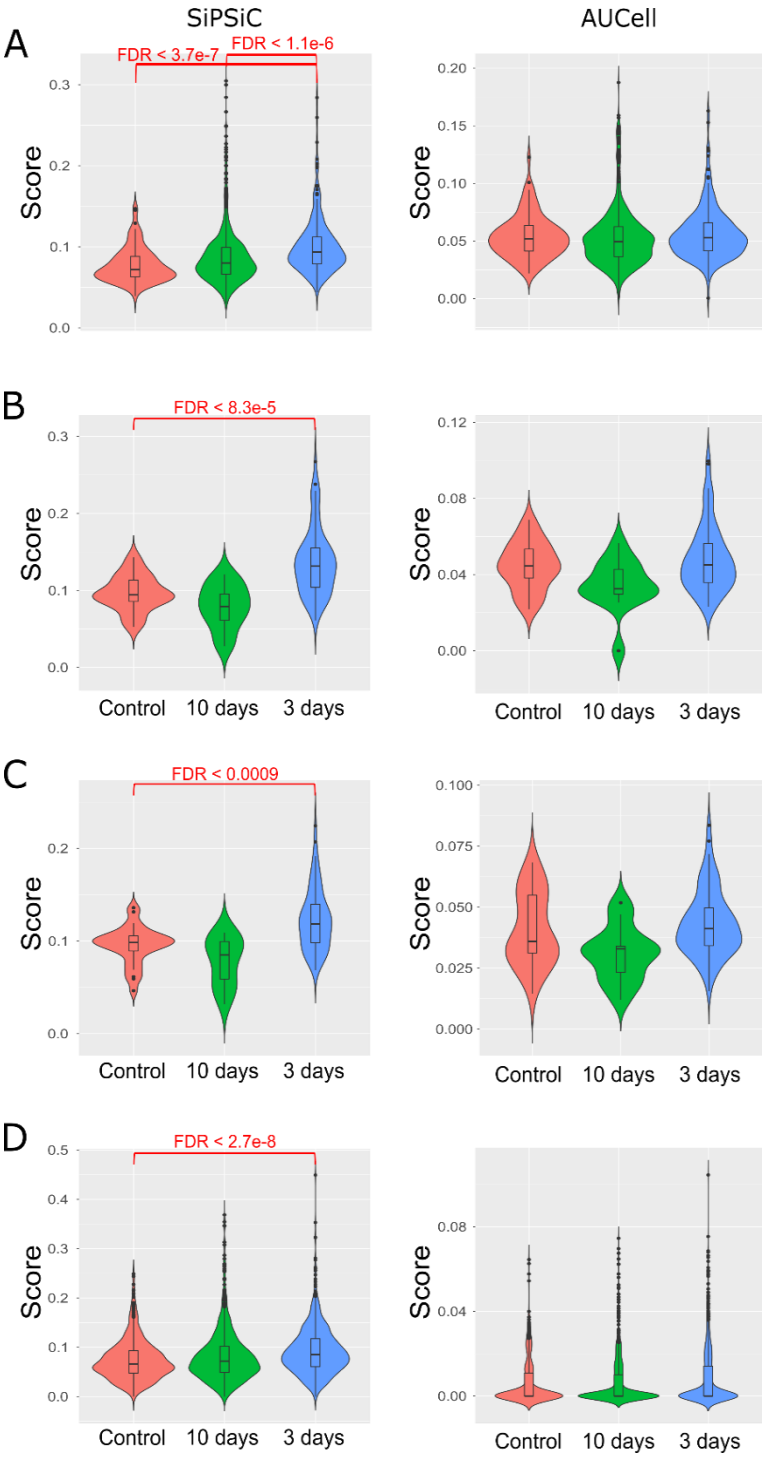

***Figure 3**. Violin plots presenting the score distribution of selected hallmark pathways for the African green monkey COVID dataset, calculated by SiPSiC (left) and AUCell (right). FDRs of T tests between significantly differential distributions are shown in red. (**A**) The complement pathway in alveolar cells. (**B**) Interferon alpha in B cells. (**C**) Interferon gamma in B cells. (**D**) MYC targets V2 in CD8+ T cells.*

Cell Type	Pathway Status	SiPSiC	AUCell	Overlap
Alveolar	Upregulated	20	9	9
	Downregulated	3	10	1
	Skipped	0	2	0
B Cells	Upregulated	2	0	0
	Downregulated	7	1	0
	Skipped	0	20	0
T Cells	Upregulated	20	11	10
	Downregulated	4	4	0
	Skipped	0	16	0

Table 1. Summary of the number of differentially expressed pathways in the active infection group of the COVID monkey dataset compared to control, both by SiPSiC and AUCell. The overlap column shows the number of pathways found as differentially expressed by both methods. Skipped pathways are pathways for which AUCell could not calculate scores. See Supplementary Table S2 for a summary of the analysis for all 50 hallmark pathways.

Cell Type	Pathway Status	SiPSiC	AUCell	Overlap
Alveolar	Upregulated	31	29	26
	Downregulated	12	9	8
	Skipped	0	4	0
B Cells	Upregulated	1	0	0
	Downregulated	0	0	0
	Skipped	0	19	0
T Cells	Upregulated	1	0	0
	Downregulated	0	0	0
	Skipped	0	24	0

Table 2. Summary of the number of differentially expressed pathways in the COVID group of the human COVID dataset compared to control, both by SiPSiC and AUCell. The overlap column shows the number of pathways found as differentially expressed by both methods. Skipped pathways are pathways for which AUCell could not calculate scores. See Supplementary Table S1 for a summary of the analysis for all 50 hallmark pathways.

SiPSiC and AUCell results for the human COVID dataset also largely agree (Table 2). Here too SiPSiC showed strong upregulation of the complement pathway in alveolar cells (FDR < $7.3*10^{-16}$), while AUCell predicts downregulation of the complement pathway with borderline statistical significance (FDR < 0.035; Figure 4A). Furthermore, as mentioned above, SiPSiC showed upregulation of TGF beta in activated B cells and the G2M checkpoint pathway in CD8+ T cells in the COVID-19 group. However, AUCell did not find any differentially active pathways.

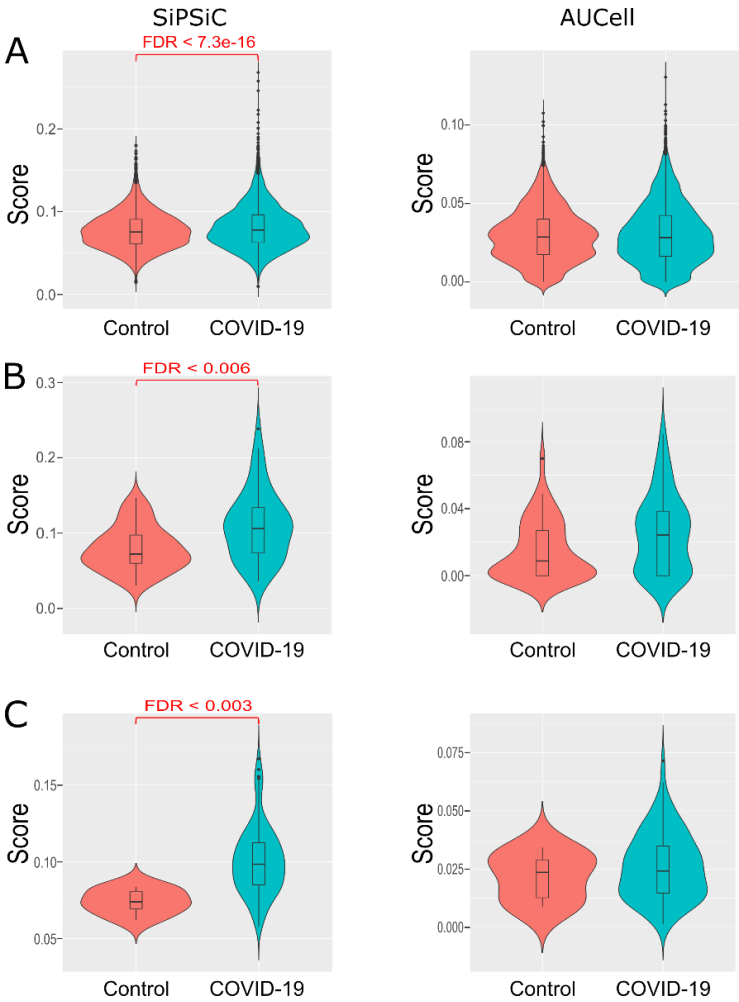

Figure 4. Violin plots presenting the score distribution of selected hallmark pathways for the human COVID dataset, calculated by SiPSiC (left) and AUCell (right). FDRs of T tests between significantly differential distributions are shown in red. (**A**) The complement pathway in alveolar cells. (**B**) TGF beta signaling in B cells. (**C**) The G2M checkpoint pathway in CD8+ T cells.

An intriguing finding is that the inflammatory response, TGFβ signaling and TNFα signaling via NFκB were all downregulated pathways in the COVID group of the human alveolar cells compared to control, both according to SiPSiC and AUCell, suggesting perhaps a counterintuitive reaction of infected epithelial cells suppressing immune response.

Comparing the results of the two methods for the glioblastoma data, we again see higher sensitivity of SiPSiC in capturing the complement pathway. Garofano et al. showed upregulation of the hallmark complement pathway in the GPM cluster of cells, which was enriched in MES-like cells. SiPSiC agrees with this finding, showing upregulation of the complement pathway in the MES-like cell state compared to all other cell states. However, AUCell found downregulation of this pathway in the MES-like state compared to the AC-like state (Figure 5A). SiPSiC also identified significant upregulation of the inflammatory response pathway (FDR < $1.2*10^{-34}$) in MES-like cells, where AUCell did not reach statistical significance comparing the MES-and AC-like cell states (p = 0.38, FDR = 0.42; Figure 5B). As stated above, the mesenchymal subtype of glioblastoma is correlated with high levels of both immune markers and infiltration of immune cells, furth er supporting these findings of SiPSiC. Furthermore, the hallmark unfolded protein response pathway is upregulated in the PPR cell cluster, which is enriched in NPC and OPC like cells. AUCell placed the MES-like cell state significantly above all other states in this pathway, and the NPC and AC-like states last, however SiPSiC placed the OPC-like state first, a statistically significant result, and the NPC-like state above the AC-like state, showing better concordance with the findings of Garofano et al (Figure 5C).

Overall, these results demonstrate that SiPSiC is more sensitive than AUCell, and is able to pick real, biologically meaningful results that AUCell misses. One major reason for this is that AUCell scores a pathway in a given cell regardless of a) the transcriptome of other cells in the data; b) the transcript counts of the different genes (as only the ranking is considered); and c) genes not in the top 5% highly expressed genes. As opposed to that, SiPSiC uses the expression of all the genes normalized by their expression across other cells (see Methods). This allows us both to utilize the information in a larger set of genes (not just the top 5%), and to be more sensitive in detecting more subtle differences (by relying on normalized expression). This is especially important if information on only a small number of genes in the gene set is available, or if many of the genes are not highly expressed, making it harder

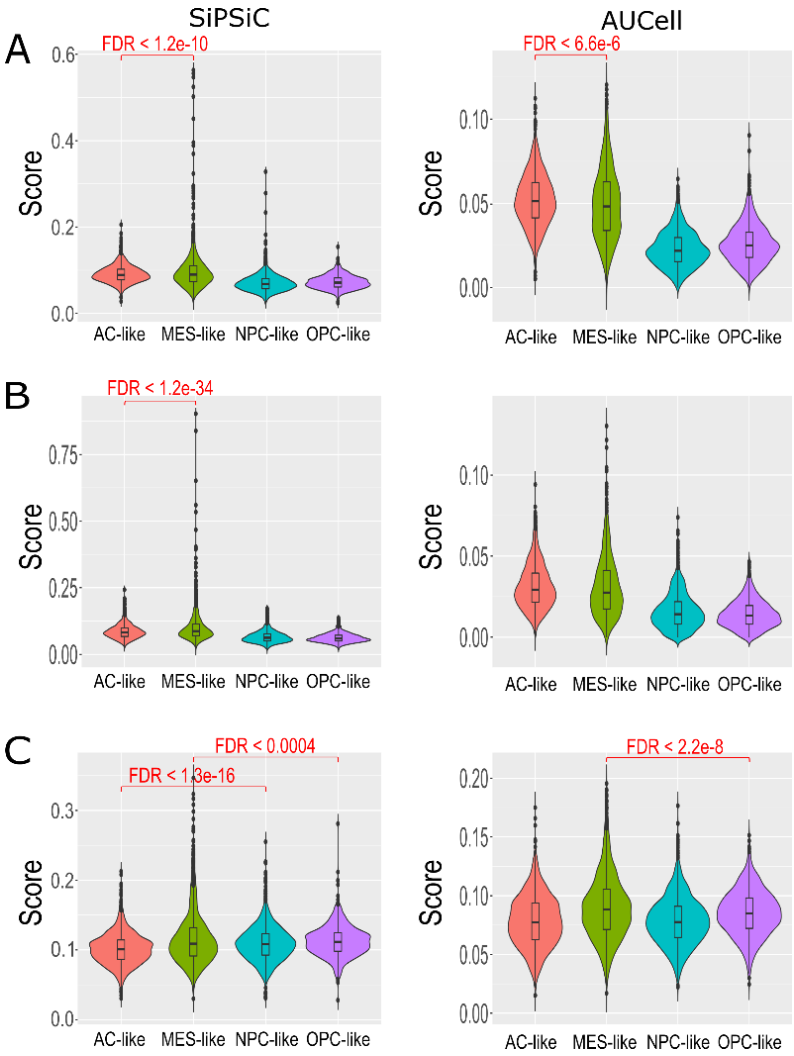

Figure 5. Score distribution of selected hallmark pathways for the glioblastoma dataset, calculated by SiPSiC (left) and AUCell (right). FDRs of T tests between significantly differential distributions are shown in red. (**A**) The complement pathway. While in SiPSiC the MES-like meta module (cell state) was higher than all other states, in AUCell it was significantly lower than the AC-like state. (**B**) The inflammatory response pathway. (**C**) The unfolded protein response pathway. AUCell placed the MES-like state above the OPC-like state, while SiPSiC placed the OPC-like state first.

to determine a robust score for this gene set. For example, when AUCell scores the MYC V2 pathway in T cells of the monkey COVID-19 dataset, the median score of both the control and COVID cell groups is zero, indicating that no genes of this pathway are among the top 5% in most cells. However, using the normalized count values of this pathway's genes in the different cells, SiPSiC managed to unveil the upregulation of the pathway in the active COVID-19 group (3-days), in accordance with prior knowledge as discussed above. A similar case is the DNA repair pathway in the alveolar cells of the human COVID dataset, where the median score of both the COVID and control cell groups is zero when scored by AUCell, whereas SiPSiC found upregulation of this pathway in the COVID group (FDR < 0.004; Supplementary Table S1), supported by previous research as mentioned above. We reason, then, that meaningful results can also be obtained by using genes that are not among the top transcribed genes, which are ignored by AUCell.

Discussion

scRNA-seq is a powerful tool to interrogate cellular heterogeneity, allowing researchers to comprehensively query changes in biological processes in high resolution. However, computational methods to infer activity of biological processes are still lacking. As scRNA-seq data are constantly being produced and shared, and as their scale and accuracy grow, it is of high value to further optimize existing methods in the field and develop novel, better ones, driving the discovery of unfamiliar biological processes and shedding light on poorly understood phenomena.

In this paper we present SiPSiC, a novel method for inferring pathway scores from scRNA-seq data. We demonstrate its high sensitivity, accuracy, and consistency with existing knowledge across different data types, including findings often missed by the original conventional analyses of these data. We demonstrate that SiPSiC scores can be used to cluster the cells and compute their UMAP projections in a manner that better captures the biological underpinnings of tissue heterogeneity. We

also show its superiority over AUCell in dissecting the functional differences between distinct groups of cells, especially when the data are sparse and partial. We reason that this superiority is attributed to the use of actual gene expression, as well as to factoring by the rank of average expression over all cells, both ignored by AUCell. To allow comparable contribution of different genes, we normalize the expression of each gene. However, to take advantage of the higher information content of highly expressed genes, the higher the total expression of a gene is, the more it contributes to the pathway score. Yet the way our algorithm works poses two potential pitfalls. First, since we use gene expression for score normalization, rather than ranks, the scores may change substantially depending on the units in which data are presented. Using logarithms of the counts, for example, is bound to change the effect size (group median differences) and statistics. Thus, based on our analyses, we recommend providing SiPSiC with TPM or CPM values and not logTPM or logCPM. Second, SiPSiC is more susceptible to outliers, again due to the use of actual gene expression values. Since the final pathway score is a weighted average of all the single gene scores, outlier scores in a fraction of the genes may pull the final score towards them, possibly leading to false positives or negatives. We therefore recommend to properly filter both genes and cells before applying SiPSiC.

Conclusions

We present SiPSiC, a novel method to infer pathway activity in single cells. SiPSiC has several advantages over existing methods for analyzing differential pathway activity. The main advantage is that it provides robust measure of pathway activity for every single cell. In addition, it can improve cell clustering and UMAP projections to capture biologically relevant differences. We demonstrate its applicability and benefits by applying it on publicly available datasets of human COVID-19 patients, African green monkeys infected with COVID-19, and glioblastoma patients. We identify multiple pathways that change their activity, many of which were not previously identified in the original papers, and reflects true biology, as is often evident from their agreement with other research studies and current knowledge on these diseases. Moreover, we suggest a novel approach to dimensional reduction and clustering by relying on SiPSiC scores instead of by gene expression. This approach emphasizes the biological similarities between cells, and reduces technical artifacts and covariates such as patient of origin. In conclusion, we demonstrate that SiPSiC can provide an accurate, comprehensive and useful understanding of biological pathway activity in single cells.

Methods

<u>The SiPSiC algorithm</u>

Taking an scRNA-seq gene expression matrix *X* in TPM or CPM, and a given gene-set, SiPSiC performs the following steps to calculate the score for all the cells in the data:

(1) **Calculate a normalization factor for each gene**: Calculate the median of the 5% cells with highest expression. If it is positive use as normalization factor, if zero use the maximum value as the normalization factor.

The reason behind this step is that scRNA-seq data are normally sparse (Chi & Deng, 2020), namely, the fraction of zeros in the data is large. Thus, by selecting the median of the top 5% cells there is a high likelihood that for most genes the value will be greater than zero, while on the other hand it will also not be an outlier, which may perturb further processing steps.

(2) **Calculate gene scores:** Rank the genes in the gene-set by their total expression (TPM or CPM values) across all cells, and divide the rank by the number of genes. Multiply by the expression and divide by the normalization factor from step 1. Therefore the gene score of gene i in cell j is $S_{i,j} =$

$X_{i,j} * rank_i / NF_i * n$, where $rank_i$ is the rank of $\sum_j X_{i,j}$, n is the number of genes in the gene set, and NF_i is the normalization factor for gene *i* calculated in step 1.

(3) **Pathway scoring**: For each cell, the gene-set score is the average gene score across all genes in the gene-set. $P_j = \sum_{i=1}^{n_P} S_{i,j} / n_P$ where n_P is the number of genes in gene-set P.

SiPSiC is available at Bioconductor (https://bioconductor.org/packages/SiPSiC) and GitHub (https://github.com/DanielDavis12/SiPSiC).

scRNA-seq datasets and processing

We downloaded published datasets from three papers (Melms et al., 2021; Neftel et al., 2019; Speranza et al., 2021). For the Human COVID dataset, cell identity annotations were downloaded as well. For the glioblastoma smart-seq2 dataset we used the malignant cell meta-module assignment that was published. To identify cell identities for the monkey COVID-19 dataset, we first identified biomarkers for alveolar, activated B, and CD8+ T cells. First, we used the human COVID-19 dataset to extract marker genes of each cell type compared to all other cells, using the FindMarkers function of Seurat (Butler et al., 2018), with logfc.threshold = 1 and min.diff.pct = 0.5, following the parameters used by Speranza et al. In addition to these markers we also selected canonical marker genes of alveolar, B and T cells from the literature: CAV1, PDPN ($T1\alpha$), SFTPB, SFTPC and SFTPD were used for alveolar cells (Chen et al., 2004), CD20, CD27, CD28 for B cells (Sanz et al., 2019) and CD2, CD8 and CXCR3 (CD138) for T cells (Groom & Luster, 2011; Tzankov et al., 2005). Next, we clustered the monkey dataset using Seurat's FindClusters function with a 0.5 resolution, and all clusters were annotated as a given cell type if and only if they displayed high expression of both the canonical markers and the markers identified in the human dataset. This resulted in 1412, 1061 and 17365 cells identified as alveolar, B, and CD8+ T cells, respectively, before filtering was applied. After filtering, these numbers dropped to 1004 (86 control, 217 3-days, and 701 10-days) alveolar cells, 113 (29 control, 71 3-days, and 13 10-days) B cells, and 2224 (360 control, 1162 3-days, and 702 10-days) T cells.

The same filtering steps were applied to the two COVID datasets and the glioblastoma smart-seq2 dataset. We first removed cells with less than 1,000 expressed genes, and then excluded genes expressed in less than 10% of the remaining cells.

For the smart-seq2 glioblastoma dataset, we used TPM / 10 provided in the original paper (multiplying the data by a constant has no effect on SiPSiC's output) for all malignant cells with reported meta-module. For the two COVID-19 datasets, we first split the data to three subsets by cell type annotation (Alveolar, B cells and CD8+ T cells) and then applied filtering, conversion to CPM and all downstream processing separately for each of these subsets.

For the glioblastoma 10X dataset, to test if SiPSiC can be used to better cluster noisy data, we used all cells and genes reported by Neftel et al. after their filtering.

Glioblastoma pathway analysis

A pathway was considered up- or down-regulated in one group compared to another if the difference of medians was > 0, or < 0, respectively, and it passed a T test with FDR < 0.01. Since the PPR and NEU clusters were enriched in both NPC- and OPC-like cells, when a specific pathway was reported as upregulated in one of these clusters, we considered our result consistent with the findings of Garofano et al. even when only one of the respective cell states (either OPC- or NPC-like) showed upregulation of that pathway. Such "semi consistent" pathways account for 5 of the 31 consistent pathways mentioned in the main text.

Clustering and cluster composition analysis

Clustering was applied to the 10X dataset published by Neftel et al. and not the smart-seq2 dataset, as the 10X dataset is much larger and has a higher proportion of non-malignant cells (9,870 malignant cells out of 16,201 cells total for the 10X dataset, whereas the smart-seq2 dataset has 6,864 malignant cells out of 7,930 total). We executed a clustering pipeline based on Seurat twice using identical parameters, first based on all genes (in the gene-based clustering) and second based on SiPSiC's pathway scores. The first 15 principal components were identified using RunPCA, and used to find the 20-nearest neighbors using FindNeighbors. Cells were clustered based on shared nearest neighbor (SNN) modularity optimization (Waltman & van Eck, 2013) using the FindClusters function with a resolution of 0.5. Cluster biomarkers (differential pathways) were identified in the pathway-based clustering, using the Wilcoxon rank sum test implemented in Seurat's FindAllMarkers function, using parameters only.pos = true, mic.pct = 0.25 and logfc.threshold = 0.05 for high sensitivity. All UMAP projections were calculated by RunUMAP based on the first 15 principal components.

We used the marker genes of Neftel et al. both for the malignant and the non-malignant cell types to annotate the cells. In both the gene-based and pathway-based analyses, cell lineage scores were calculated using SiPSiC to ensure that the same annotations are used. For the NPC-like meta-module, Neftel et al. provided two different sets of marker genes named NPClike1 and NPClike2 (referred to in the results section as the first and second NPC-like marker gene sets, respectively), reflecting the two sub-types of this meta-module. For the malignant cell types, cells with scores higher than 0.13 were annotated as belonging to the lineage for which they got this score, whereas in the case of T cells and macrophages a threshold of 0.05 was used.

Acknowledgments

We thank Michal Rabani, Michael Berger and Mor Nitzan (HUJI) for their insightful comments on the manuscript. This work was supported by the European Research Council Horizon 2020 grant 949029 (YD), and the Israel Science Foundation grant 3650/20 (YD).

References

Abu-Farha, M., Thanaraj, T. A., Qaddoumi, M. G., Hashem, A., Abubaker, J., & Al-Mulla, F. (2020). The Role of Lipid Metabolism in COVID-19 Virus Infection and as a Drug Target. *International Journal of Molecular Sciences*, *21*(10), 3544. https://doi.org/10.3390/ijms21103544

Ackermann, M., Verleden, S. E., Kuehnel, M., Haverich, A., Welte, T., Laenger, F., Vanstapel, A., Werlein, C., Stark, H., Tzankov, A., Li, W. W., Li, V. W., Mentzer, S. J., & Jonigk, D. (2020). Pulmonary Vascular Endothelialitis, Thrombosis, and Angiogenesis in Covid-19. *New England Journal of Medicine*, *383*(2), 120–128. https://doi.org/10.1056/NEJMoa2015432

Afzali, B., Noris, M., Lambrecht, B. N., & Kemper, C. (2021). The state of complement in COVID-19. *Nature Reviews Immunology 2021 22:2*, *22*(2), 77–84. https://doi.org/10.1038/s41577-021-00665-1

Aibar, S., González-Blas, C. B., Moerman, T., Huynh-Thu, V. A., Imrichova, H., Hulselmans, G., Rambow, F., Marine, J.-C., Geurts, P., Aerts, J., van den Oord, J., Atak, Z. K., Wouters, J., & Aerts, S. (2017). SCENIC: single-cell regulatory network inference and clustering. *Nature Methods*, *14*(11), 1083–1086. https://doi.org/10.1038/nmeth.4463

Angeles-Floriano, T., Sanjuan-Méndez, A., Rivera-Torruco, G., Parra-Ortega, I., Lopez-Martinez, B., Martinez-Castro, J., Marin-Santiago, S., Alcántara-Hernández, C., Martínez-Martínez, A.,

Márquez-González, H., Klünder-Klünder, M., Olivar-López, V., Zaragoza-Ojeda, M., Arenas-Huertero, F., Torres-Aguilar, H., Medina-Contreras, O., Zlotnik, A., & Valle-Rios, R. (2023). Leukocyte surface expression of the endoplasmic reticulum chaperone GRP78 is increased in severe COVID-19. *Journal of Leukocyte Biology*, *113*(1), 1–10. https://doi.org/10.1093/jleuko/qiac017

Appelberg, S., Gupta, S., Svensson Akusjärvi, S., Ambikan, A. T., Mikaeloff, F., Saccon, E., Végvári, Á., Benfeitas, R., Sperk, M., Ståhlberg, M., Krishnan, S., Singh, K., Penninger, J. M., Mirazimi, A., & Neogi, U. (2020). Dysregulation in Akt/mTOR/HIF-1 signaling identified by proteo-transcriptomics of SARS-CoV-2 infected cells. *Emerging Microbes & Infections*, *9*(1), 1748–1760. https://doi.org/10.1080/22221751.2020.1799723

Bhat, K. P. L., Balasubramaniyan, V., Vaillant, B., Ezhilarasan, R., Hummelink, K., Hollingsworth, F., Wani, K., Heathcock, L., James, J. D., Goodman, L. D., Conroy, S., Long, L., Lelic, N., Wang, S., Gumin, J., Raj, D., Kodama, Y., Raghunathan, A., Olar, A., … Aldape, K. (2013). Mesenchymal Differentiation Mediated by NF-κB Promotes Radiation Resistance in Glioblastoma. *Cancer Cell*, *24*(3), 331–346. https://doi.org/10.1016/j.ccr.2013.08.001

Blum, R., Jacob-Hirsch, J., Amariglio, N., Rechavi, G., & Kloog, Y. (2005). Ras Inhibition in Glioblastoma Down-regulates Hypoxia-Inducible Factor-1α, Causing Glycolysis Shutdown and Cell Death. *Cancer Research*, *65*(3), 999–1006. https://doi.org/10.1158/0008-5472.999.65.3

Bojkova, D., Klann, K., Koch, B., Widera, M., Krause, D., Ciesek, S., Cinatl, J., & Münch, C. (2020). Proteomics of SARS-CoV-2-infected host cells reveals therapy targets. *Nature*, *583*(7816), 469–472. https://doi.org/10.1038/s41586-020-2332-7

Bordoni, V., Tartaglia, E., Sacchi, A., Fimia, G. M., Cimini, E., Casetti, R., Notari, S., Grassi, G., Marchioni, L., Bibas, M., Capobianchi, M. R., Locatelli, F., Maeurer, M., Zumla, A., Antinori, A., Nicastri, E., Ippolito, G., & Agrati, C. (2021). The unbalanced p53/SIRT1 axis may impact lymphocyte homeostasis in COVID-19 patients. *International Journal of Infectious Diseases*, *105*, 49–53. https://doi.org/10.1016/j.ijid.2021.02.019

Butler, A., Hoffman, P., Smibert, P., Papalexi, E., & Satija, R. (2018). Integrating single-cell transcriptomic data across different conditions, technologies, and species. *Nature Biotechnology*, *36*(5), 411–420. https://doi.org/10.1038/nbt.4096

Chen, Z., Jin, N., Narasaraju, T., Chen, J., McFarland, L. R., Scott, M., & Liu, L. (2004). Identification of two novel markers for alveolar epithelial type I and II cells. *Biochemical and Biophysical Research Communications*, *319*(3), 774–780. https://doi.org/10.1016/j.bbrc.2004.05.048

Chi, W., & Deng, M. (2020). Sparsity-Penalized Stacked Denoising Autoencoders for Imputing Single-Cell RNA-seq Data. *Genes*, *11*(5), 532. https://doi.org/10.3390/genes11050532

Choi, E. Y., Park, H. H., Kim, H., Kim, H. N., Kim, I., Jeon, S., Kim, W., Bae, J.-S., & Lee, W. (2020). Wnt5a and Wnt11 as acute respiratory distress syndrome biomarkers for severe acute respiratory syndrome coronavirus 2 patients. *European Respiratory Journal*, *56*(5), 2001531. https://doi.org/10.1183/13993003.01531-2020

Codo, A. C., Davanzo, G. G., Monteiro, L. de B., de Souza, G. F., Muraro, S. P., Virgilio-da-Silva, J. V., Prodonoff, J. S., Carregari, V. C., de Biagi Junior, C. A. O., Crunfli, F., Jimenez Restrepo, J. L., Vendramini, P. H., Reis-de-Oliveira, G., Bispo dos Santos, K., Toledo-Teixeira, D. A., Parise, P. L., Martini, M. C., Marques, R. E., Carmo, H. R., … Moraes-Vieira, P. M. (2020). Elevated Glucose

Levels Favor SARS-CoV-2 Infection and Monocyte Response through a HIF-1α/Glycolysis-Dependent Axis. *Cell Metabolism*, *32*(3), 437-446.e5. https://doi.org/10.1016/j.cmet.2020.07.007

Drier, Y., Sheffer, M., & Domany, E. (2013). Pathway-based personalized analysis of cancer. *Proceedings of the National Academy of Sciences of the United States of America*, *110*(16), 6388–6393. https://doi.org/10.1073/pnas.1219651110

Düvel, K., Yecies, J. L., Menon, S., Raman, P., Lipovsky, A. I., Souza, A. L., Triantafellow, E., Ma, Q., Gorski, R., Cleaver, S., Vander Heiden, M. G., MacKeigan, J. P., Finan, P. M., Clish, C. B., Murphy, L. O., & Manning, B. D. (2010). Activation of a Metabolic Gene Regulatory Network Downstream of mTOR Complex 1. *Molecular Cell*, *39*(2), 171–183. https://doi.org/10.1016/j.molcel.2010.06.022

Echavarría-Consuegra, L., Cook, G. M., Busnadiego, I., Lefèvre, C., Keep, S., Brown, K., Doyle, N., Dowgier, G., Franaszek, K., Moore, N. A., Siddell, S. G., Bickerton, E., Hale, B. G., Firth, A. E., Brierley, I., & Irigoyen, N. (2021). Manipulation of the unfolded protein response: A pharmacological strategy against coronavirus infection. *PLOS Pathogens*, *17*(6), e1009644. https://doi.org/10.1371/journal.ppat.1009644

Engler, J. R., Robinson, A. E., Smirnov, I., Hodgson, J. G., Berger, M. S., Gupta, N., James, C. D., Molinaro, A., & Phillips, J. J. (2012). Increased Microglia/Macrophage Gene Expression in a Subset of Adult and Pediatric Astrocytomas. *PLoS ONE*, *7*(8), e43339. https://doi.org/10.1371/journal.pone.0043339

Ferreira-Gomes, M., Kruglov, A., Durek, P., Heinrich, F., Tizian, C., Heinz, G. A., Pascual-Reguant, A., Du, W., Mothes, R., Fan, C., Frischbutter, S., Habenicht, K., Budzinski, L., Ninnemann, J., Jani, P. K., Guerra, G. M., Lehmann, K., Matz, M., Ostendorf, L., … Mashreghi, M. F. (2021). SARS-CoV-2 in severe COVID-19 induces a TGF-β-dominated chronic immune response that does not target itself. *Nature Communications 2021 12:1*, *12*(1), 1–14. https://doi.org/10.1038/s41467-021-22210-3

Garcia, G., Sharma, A., Ramaiah, A., Sen, C., Purkayastha, A., Kohn, D. B., Parcells, M. S., Beck, S., Kim, H., Bakowski, M. A., Kirkpatrick, M. G., Riva, L., Wolff, K. C., Han, B., Yuen, C., Ulmert, D., Purbey, P. K., Scumpia, P., Beutler, N., … Arumugaswami, V. (2021). Antiviral drug screen identifies DNA-damage response inhibitor as potent blocker of SARS-CoV-2 replication. *Cell Reports*, *35*(1), 108940. https://doi.org/10.1016/j.celrep.2021.108940

Garofano, L., Migliozzi, S., Oh, Y. T., D'Angelo, F., Najac, R. D., Ko, A., Frangaj, B., Caruso, F. P., Yu, K., Yuan, J., Zhao, W., Luisa Di Stefano, A., Bielle, F., Jiang, T., Sims, P., Suvà, M. L., Tang, F., Su, X. D., Ceccarelli, M., … Iavarone, A. (2021). Pathway-based classification of glioblastoma uncovers a mitochondrial subtype with therapeutic vulnerabilities. *Nature Cancer*, *2*(2), 141–156. https://doi.org/10.1038/s43018-020-00159-4

Gioia, U., Tavella, S., Martínez-Orellana, P., Cicio, G., Colliva, A., Ceccon, M., Cabrini, M., Henriques, A. C., Fumagalli, V., Paldino, A., Presot, E., Rajasekharan, S., Iacomino, N., Pisati, F., Matti, V., Sepe, S., Conte, M. I., Barozzi, S., Lavagnino, Z., … d'Adda di Fagagna, F. (2023). SARS-CoV-2 infection induces DNA damage, through CHK1 degradation and impaired 53BP1 recruitment, and cellular senescence. *Nature Cell Biology*, *25*(4), 550–564. https://doi.org/10.1038/s41556-023-01096-x

Gnanaprakasam, J. N., & Wang, R. (2017). MYC in Regulating Immunity: Metabolism and Beyond. *Genes*, *8*(3), 88. https://doi.org/10.3390/genes8030088

Groom, J. R., & Luster, A. D. (2011). CXCR3 in T cell function. *Experimental Cell Research*, *317*(5), 620–631. https://doi.org/10.1016/j.yexcr.2010.12.017

Han, H., Ma, Q., Li, C., Liu, R., Zhao, L., Wang, W., Zhang, P., Liu, X., Gao, G., Liu, F., Jiang, Y., Cheng, X., Zhu, C., & Xia, Y. (2020). Profiling serum cytokines in COVID-19 patients reveals IL-6 and IL-10 are disease severity predictors. *Emerging Microbes & Infections*, *9*(1), 1123–1130. https://doi.org/10.1080/22221751.2020.1770129

Hänzelmann, S., Castelo, R., & Guinney, J. (2013). GSVA: gene set variation analysis for microarray and RNA-seq data. *BMC Bioinformatics*, *14*, 7. https://doi.org/10.1186/1471-2105-14-7

Iser, I. C., Pereira, M. B., Lenz, G., & Wink, M. R. (2017). The Epithelial-to-Mesenchymal Transition-Like Process in Glioblastoma: An Updated Systematic Review and In Silico Investigation. *Medicinal Research Reviews*, *37*(2), 271–313. https://doi.org/10.1002/med.21408

Izquierdo, J. L., Soriano, J. B., González, Y., Lumbreras, S., Ancochea, J., Echeverry, C., & Rodríguez, J. M. (2022). Use of N-Acetylcysteine at high doses as an oral treatment for patients hospitalized with COVID-19. *Science Progress*, *105*(1), 003685042210745. https://doi.org/10.1177/00368504221074574

Jafarzadeh, A., Nemati, M., & Jafarzadeh, S. (2021). Contribution of STAT3 to the pathogenesis of COVID-19. *Microbial Pathogenesis*, *154*, 104836. https://doi.org/10.1016/j.micpath.2021.104836

John, G. R., Shankar, S. L., Shafit-Zagardo, B., Massimi, A., Lee, S. C., Raine, C. S., & Brosnan, C. F. (2002). Multiple sclerosis: Re-expression of a developmental pathway that restricts oligodendrocyte maturation. *Nature Medicine*, *8*(10), 1115–1121. https://doi.org/10.1038/nm781

Kato, H., Nakajima, S., Saito, Y., Takahashi, S., Katoh, R., & Kitamura, M. (2012). mTORC1 serves ER stress-triggered apoptosis via selective activation of the IRE1–JNK pathway. *Cell Death & Differentiation*, *19*(2), 310–320. https://doi.org/10.1038/cdd.2011.98

Kim, H., Choi, J.-A., & Kim, J.-H. (2014). Ras Promotes Transforming Growth Factor-β (TGF-β)-induced Epithelial-Mesenchymal Transition via a Leukotriene B4 Receptor-2-linked Cascade in Mammary Epithelial Cells. *Journal of Biological Chemistry*, *289*(32), 22151–22160. https://doi.org/10.1074/jbc.M114.556126

Klann, K., Bojkova, D., Tascher, G., Ciesek, S., Münch, C., & Cinatl, J. (2020). Growth Factor Receptor Signaling Inhibition Prevents SARS-CoV-2 Replication. *Molecular Cell*, *80*(1), 164-174.e4. https://doi.org/10.1016/j.molcel.2020.08.006

Korotkevich, G., Sukhov, V., Budin, N., Shpak, B., Artyomov, M. N., & Sergushichev, A. (2021). Fast gene set enrichment analysis. *BioRxiv*, 060012. https://doi.org/10.1101/060012

Lamouille, S., Xu, J., & Derynck, R. (2014). Molecular mechanisms of epithelial–mesenchymal transition. *Nature Reviews Molecular Cell Biology*, *15*(3), 178–196. https://doi.org/10.1038/nrm3758

Lee, C. (2018). Therapeutic Modulation of Virus-Induced Oxidative Stress via the Nrf2-Dependent Antioxidative Pathway. *Oxidative Medicine and Cellular Longevity*, *2018*, 1–26. https://doi.org/10.1155/2018/6208067

Liao, M., Liu, Y., Yuan, J., Wen, Y., Xu, G., Zhao, J., Cheng, L., Li, J., Wang, X., Wang, F., Liu, L., Amit, I., Zhang, S., & Zhang, Z. (2020). Single-cell landscape of bronchoalveolar immune cells in patients with COVID-19. *Nature Medicine*, *26*(6), 842–844. https://doi.org/10.1038/s41591-020-0901-9

Liberzon, A., Birger, C., Thorvaldsdóttir, H., Ghandi, M., Mesirov, J. P., & Tamayo, P. (2015). The Molecular Signatures Database Hallmark Gene Set Collection. *Cell Systems*, *1*(6), 417–425. https://doi.org/10.1016/j.cels.2015.12.004

Liu, S., Zhang, C., Wang, B., Zhang, H., Qin, G., Li, C., Cao, L., Gao, Q., Ping, Y., Zhang, K., Lian, J., Zhao, Q., Wang, D., Zhang, Z., Zhao, X., Yang, L., Huang, L., Yang, B., & Zhang, Y. (2021). Regulatory T cells promote glioma cell stemness through TGF-β–NF-κB–IL6–STAT3 signaling. *Cancer Immunology, Immunotherapy*, *70*(9), 2601–2616. https://doi.org/10.1007/s00262-021-02872-0

Marques, C., Unterkircher, T., Kroon, P., Oldrini, B., Izzo, A., Dramaretska, Y., Ferrarese, R., Kling, E., Schnell, O., Nelander, S., Wagner, E. F., Bakiri, L., Gargiulo, G., Carro, M. S., & Squatrito, M. (2021). NF1 regulates mesenchymal glioblastoma plasticity and aggressiveness through the AP-1 transcription factor FOSL1. *ELife*, *10*. https://doi.org/10.7554/eLife.64846

Melms, J. C., Biermann, J., Huang, H., Wang, Y., Nair, A., Tagore, S., Katsyv, I., Rendeiro, A. F., Amin, A. D., Schapiro, D., Frangieh, C. J., Luoma, A. M., Filliol, A., Fang, Y., Ravichandran, H., Clausi, M. G., Alba, G. A., Rogava, M., Chen, S. W., … Izar, B. (2021). A molecular single-cell lung atlas of lethal COVID-19. *Nature*, *595*(7865), 114–119. https://doi.org/10.1038/s41586-021-03569-1

Muñoz-Fontela, C., Macip, S., Martínez-Sobrido, L., Brown, L., Ashour, J., García-Sastre, A., Lee, S. W., & Aaronson, S. A. (2008). Transcriptional role of p53 in interferon-mediated antiviral immunity. *Journal of Experimental Medicine*, *205*(8), 1929–1938. https://doi.org/10.1084/jem.20080383

Neftel, C., Laffy, J., Filbin, M. G., Hara, T., Shore, M. E., Rahme, G. J., Richman, A. R., Silverbush, D., Shaw, M. L., Hebert, C. M., Dewitt, J., Gritsch, S., Perez, E. M., Gonzalez Castro, L. N., Lan, X., Druck, N., Rodman, C., Dionne, D., Kaplan, A., … Suvà, M. L. (2019). An Integrative Model of Cellular States, Plasticity, and Genetics for Glioblastoma. *Cell*, *178*(4), 835-849.e21. https://doi.org/10.1016/j.cell.2019.06.024

Noureen, N., Ye, Z., Chen, Y., Wang, X., & Zheng, S. (2022). Signature-scoring methods developed for bulk samples are not adequate for cancer single-cell RNA sequencing data. *ELife* , *11*(e71994). https://doi.org/10.7554/eLife

Patra, T., Meyer, K., Geerling, L., Isbell, T. S., Hoft, D. F., Brien, J., Pinto, A. K., Ray, R. B., & Ray, R. (2020). SARS-CoV-2 spike protein promotes IL-6 trans-signaling by activation of angiotensin II receptor signaling in epithelial cells. *PLOS Pathogens*, *16*(12), e1009128. https://doi.org/10.1371/journal.ppat.1009128

Puzyrenko, A., Jacobs, E. R., Sun, Y., Felix, J. C., Sheinin, Y., Ge, L., Lai, S., Dai, Q., Gantner, B. N., Nanchal, R., North, P. E., Simpson, P. M., Rui, H., & Benjamin, I. J. (2021). Pneumocytes are distinguished by highly elevated expression of the ER stress biomarker GRP78, a co-receptor for SARS-CoV-2, in COVID-19 autopsies. *Cell Stress and Chaperones*, *26*(5), 859–868. https://doi.org/10.1007/s12192-021-01230-4

Ren, Y., Shu, T., Wu, D., Mu, J., Wang, C., Huang, M., Han, Y., Zhang, X.-Y., Zhou, W., Qiu, Y., & Zhou, X. (2020). The ORF3a protein of SARS-CoV-2 induces apoptosis in cells. *Cellular & Molecular Immunology*, *17*(8), 881–883. https://doi.org/10.1038/s41423-020-0485-9

Rizzo, P., Vieceli Dalla Sega, F., Fortini, F., Marracino, L., Rapezzi, C., & Ferrari, R. (2020). COVID-19 in the heart and the lungs: could we "Notch" the inflammatory storm? *Basic Research in Cardiology*, *115*(3), 31. https://doi.org/10.1007/s00395-020-0791-5

Sanli, D. E. T., Altundag, A., Kandemirli, S. G., Yildirim, D., Sanli, A. N., Saatci, O., Kirisoglu, C. E., Dikensoy, O., Murrja, E., Yesil, A., Bastan, S., Karsidag, T., Akinci, I. O., Ozkok, S., Yilmaz, E., Tuzuner, F., Kilercik, M., & Ljama, T. (2021). Relationship between disease severity and serum IL-6 levels in COVID-19 anosmia. *American Journal of Otolaryngology*, *42*(1), 102796. https://doi.org/10.1016/j.amjoto.2020.102796

Sanz, I., Wei, C., Jenks, S. A., Cashman, K. S., Tipton, C., Woodruff, M. C., Hom, J., & Lee, F. E.-H. (2019). Challenges and Opportunities for Consistent Classification of Human B Cell and Plasma Cell Populations. *Frontiers in Immunology*, *10*. https://doi.org/10.3389/fimmu.2019.02458

Schultheiß, C., Paschold, L., Simnica, D., Mohme, M., Willscher, E., von Wenserski, L., Scholz, R., Wieters, I., Dahlke, C., Tolosa, E., Sedding, D. G., Ciesek, S., Addo, M., & Binder, M. (2020). Next-Generation Sequencing of T and B Cell Receptor Repertoires from COVID-19 Patients Showed Signatures Associated with Severity of Disease. *Immunity*, *53*(2), 442-455.e4. https://doi.org/10.1016/J.IMMUNI.2020.06.024

Speranza, E., Williamson, B. N., Feldmann, F., Sturdevant, G. L., Pérez-Pérez, L., Meade-White, K., Smith, B. J., Lovaglio, J., Martens, C., Munster, V. J., Okumura, A., Shaia, C., Feldmann, H., Best, S. M., & de Wit, E. (2021). Single-cell RNA sequencing reveals SARS-CoV-2 infection dynamics in lungs of African green monkeys. In *Sci. Transl. Med* (Vol. 13). http://stm.sciencemag.org/

Sprooten, J., & Garg, A. D. (2020). *Type I interferons and endoplasmic reticulum stress in health and disease* (pp. 63–118). https://doi.org/10.1016/bs.ircmb.2019.10.004

Stukalov, A., Girault, V., Grass, V., Karayel, O., Bergant, V., Urban, C., Haas, D. A., Huang, Y., Oubraham, L., Wang, A., Hamad, M. S., Piras, A., Hansen, F. M., Tanzer, M. C., Paron, I., Zinzula, L., Engleitner, T., Reinecke, M., Lavacca, T. M., … Pichlmair, A. (2021). Multilevel proteomics reveals host perturbations by SARS-CoV-2 and SARS-CoV. *Nature*, *594*(7862), 246–252. https://doi.org/10.1038/s41586-021-03493-4

Takaoka, A., Hayakawa, S., Yanai, H., Stoiber, D., Negishi, H., Kikuchi, H., Sasaki, S., Imai, K., Shibue, T., Honda, K., & Taniguchi, T. (2003). Integration of interferon-α/β signalling to p53 responses in tumour suppression and antiviral defence. *Nature*, *424*(6948), 516–523. https://doi.org/10.1038/nature01850

Tzankov, A., Bourgau, C., Kaiser, A., Zimpfer, A., Maurer, R., Pileri, S. A., Went, P., & Dirnhofer, S. (2005). Rare expression of T-cell markers in classical Hodgkin's lymphoma. *Modern Pathology*, *18*(12), 1542–1549. https://doi.org/10.1038/modpathol.3800473

Verhaak, R. G. W., Hoadley, K. A., Purdom, E., Wang, V., Qi, Y., Wilkerson, M. D., Miller, C. R., Ding, L., Golub, T., Mesirov, J. P., Alexe, G., Lawrence, M., O'Kelly, M., Tamayo, P., Weir, B. A., Gabriel, S., Winckler, W., Gupta, S., Jakkula, L., … Hayes, D. N. (2010). An integrated genomic analysis identifies clinically relevant subtypes of glioblastoma characterized by abnormalities in

PDGFRA, IDH1, EGFR and NF1. *Cancer Cell*, *17*(1), 98. https://doi.org/10.1016/J.CCR.2009.12.020

Waltman, L., & van Eck, N. J. (2013). A smart local moving algorithm for large-scale modularity-based community detection. *The European Physical Journal B*, *86*(11), 471. https://doi.org/10.1140/epjb/e2013-40829-0

Wang, C., Zhang, C.-J., Martin, B. N., Bulek, K., Kang, Z., Zhao, J., Bian, G., Carman, J. A., Gao, J., Dongre, A., Xue, H., Miller, S. D., Qian, Y., Hambardzumyan, D., Hamilton, T., Ransohoff, R. M., & Li, X. (2017). IL-17 induced NOTCH1 activation in oligodendrocyte progenitor cells enhances proliferation and inflammatory gene expression. *Nature Communications*, *8*(1), 15508. https://doi.org/10.1038/ncomms15508

Wang, H., Cai, H., Ao, L., Yan, H., Zhao, W., Qi, L., Gu, Y., & Guo, Z. (2016). Individualized identification of disease-associated pathways with disrupted coordination of gene expression. *Briefings in Bioinformatics*, *17*(1), 78–87. https://doi.org/10.1093/bib/bbv030

Wang, Q., Hu, B., Hu, X., Kim, H., Squatrito, M., Scarpace, L., deCarvalho, A. C., Lyu, S., Li, P., Li, Y., Barthel, F., Cho, H. J., Lin, Y. H., Satani, N., Martinez-Ledesma, E., Zheng, S., Chang, E., Sauvé, C. E. G., Olar, A., … Verhaak, R. G. W. (2017). Tumor Evolution of Glioma-Intrinsic Gene Expression Subtypes Associates with Immunological Changes in the Microenvironment. *Cancer Cell*, *32*(1), 42-56.e6. https://doi.org/10.1016/j.ccell.2017.06.003

Wang, S., Sdrulla, A. D., diSibio, G., Bush, G., Nofziger, D., Hicks, C., Weinmaster, G., & Barres, B. A. (1998). Notch Receptor Activation Inhibits Oligodendrocyte Differentiation. *Neuron*, *21*(1), 63–75. https://doi.org/10.1016/S0896-6273(00)80515-2

Williams, C. G., Jureka, A. S., Silvas, J. A., Nicolini, A. M., Chvatal, S. A., Carlson-Stevermer, J., Oki, J., Holden, K., & Basler, C. F. (2021). Inhibitors of VPS34 and fatty-acid metabolism suppress SARS-CoV-2 replication. *Cell Reports*, *36*(5), 109479. https://doi.org/10.1016/j.celrep.2021.109479

Yan, T., Tan, Y., Deng, G., Sun, Z., Liu, B., Wang, Y., Yuan, F., Sun, Q., Hu, P., Gao, L., Tian, D., & Chen, Q. (2022). TGF-β induces GBM mesenchymal transition through upregulation of CLDN4 and nuclear translocation to activate TNF-α/NF-κB signal pathway. *Cell Death & Disease*, *13*(4), 339. https://doi.org/10.1038/s41419-022-04788-8

Yuen, C., Wong, W., Mak, L., Wang, X., Chu, H., Yuen, K., & Kok, K. (2021). Suppression of SARS-CoV-2 infection in ex-vivo human lung tissues by targeting class III phosphoinositide 3-kinase. *Journal of Medical Virology*, *93*(4), 2076–2083. https://doi.org/10.1002/jmv.26583

Zhang, L., Wang, H., Zhu, J., Ding, K., & Xu, J. (2014). FTY720 reduces migration and invasion of human glioblastoma cell lines via inhibiting the PI3K/AKT/mTOR/p70S6K signaling pathway. *Tumor Biology*, *35*(11), 10707–10714. https://doi.org/10.1007/s13277-014-2386-y

Zhao, Y., Kang, J.-H., Yoo, K.-C., Kang, S.-G., Lee, H.-J., & Lee, S.-J. (2021). K-RAS Acts as a Critical Regulator of CD44 to Promote the Invasiveness and Stemness of GBM in Response to Ionizing Radiation. *International Journal of Molecular Sciences*, *22*(20), 10923. https://doi.org/10.3390/ijms222010923

Zhu, N., Wang, W., Liu, Z., Liang, C., Wang, W., Ye, F., Huang, B., Zhao, L., Wang, H., Zhou, W., Deng, Y., Mao, L., Su, C., Qiang, G., Jiang, T., Zhao, J., Wu, G., Song, J., & Tan, W. (2020). Morphogenesis and cytopathic effect of SARS-CoV-2 infection in human airway epithelial cells. *Nature Communications*, *11*(1), 3910. https://doi.org/10.1038/s41467-020-17796-z